國家科學及技術委員會補助專題研究計畫報告

標靶整合素αvβ3-FAK訊號網絡的膽管癌診療策略開發-標靶膽管癌整合素αvβ3訊號網絡的新型診療性奈米微脂體DL-N2之研究(3/3)

報 告 類 別 ： 成果報告
計 畫 類 別 ： 整合型計畫
計 畫 編 號 ： NSTC 112-2314-B-038-004-
執 行 期 間 ： 112年08月01日至113年10月31日
執 行 單 位 ： 臺北醫學大學癌症生物學與藥物研發研究所

計 畫 主 持 人： 林宏惲
共 同 主 持 人： 何意

計畫參與人員： 碩士級-專任助理：李姿霖
三專級-專任助理：莫汝谷
其他-其他：施雅蓉
博士後研究-博士後研究：蔡仲哲
其他-兼任助理：沈芯羽

報 告 附 件 ： 出席國際學術會議心得報告

本研究具有政策應用參考價值：■否 □是，建議提供機關
（勾選「是」者，請列舉建議可提供施政參考之業務主管機關）
本研究具影響公共利益之重大發現：□否 □是

中 華 民 國 114 年 01 月 23 日

中 文 摘 要 ： 表皮生長因子（EGF）與其表面受體結合，刺激基因表現和癌細胞增生。 EGF 透過 PI3K 和程序性細胞死亡配體 1（PD-L1）途徑刺激癌細胞生長。整合素 αvβ3 拮抗劑，heteronemin在癌細胞中表現出有效的細胞毒性作用。它抑制 EGF 促進的關鍵訊號傳導途徑。在本研究中，我們研究了EGF誘導的膽管癌細胞訊號活化和增殖效應，並進一步探討了其分子標靶。 Heteronemin 逆轉 EGF 的作用，並透過 PI3K 活性阻斷進一步增強。總之，EGF 刺激膽管癌的細胞生長。另一方面，heteronemin 抑制 PI3K 活化和 PD-L1 表達，從而逆轉 EGF 誘導的膽管癌細胞基因表現和增殖的刺激作用。異種移植研究還顯示，奈米脂質藥物（DL-N2）透過抑制整合素 αvβ3 網路活動包括 EGF 依賴性訊號傳導途徑來抑制膽管癌的生長。

中 文 關 鍵 詞 ： 程式化死亡配體1、表皮生長因子、膽管癌、海綿素、四碘甲狀腺乙酸衍生物

英 文 摘 要 ： Epidermal growth factor (EGF) binds with its surface receptors to stimulate gene expression and cancer cell proliferation. EGF stimulated cancer cell growth via PI3K and programmed cell death ligand 1 (PD-L1) pathways. As an integrin αvβ3 antagonist, heteronemin exhibits potent cytotoxic effects in cancer cells. It inhibited critical signal transduction pathways promoted by EGF. In the current study, we investigated EGF-induced signal activation and proliferation effects in cholangiocarcinoma cells and further explored its molecular targets. Heteronemin reversed the effects of EGF and was further enhanced by PI3K activity blockage. Thus, EGF stimulated cell growth in cholangiocarcinoma. Interfering with integrin αvβ3 activities inhibited PI3K activation and PD-L1 expression to reverse the stimulatory effects of EGF-induced gene expression and proliferation in cholangiocarcinoma cells. Xenografted studies also indicated that nano-lipo-drug (DL-N2) inhibited cholangiocarcinoma cancer growth via inhibiting integrin αvβ3 network activities, including EGF-dependent signal transduction pathways.

英 文 關 鍵 詞 ： Programmed death-ligand 1, Epidermal growth factors, Cholangiocarcinoma, Heteronemin, Tetrac derivatives

INTRODUCTION

Cholangiocarcinomas are aggressive biliary neoplasms arising within the intrahepatic or extrahepatic biliary tract. They are the second most common type of primary liver cancer [1]. An increasing incidence of cholangiocarcinoma has been documented. The incidence of cholangiocarcinoma is rising, contributing to high mortality rates due to the lack of effective therapeutic options. One-third of intrahepatic cholangiocarcinomas exhibit mutant *KRAS* and aberrant p53 expression [2]. These mutations confer resistance to many chemotherapeutic agents in cholangiocarcinomas, yet there is currently no standard therapy for this scenario [3, 4]. Fifteen percent of the *epidermal growth factor receptor* (*EGFR*) gene mutations in the kinase domain are in biliary cancer [5]. Fifty percent of cholangiocarcinomas feature overexpressed EGFR and cytoplasmic localization of E-cadherin, correlating with the presence of satellite nodules and peripheral types of cancers [6]. In vitro studies reveal that EGF induces scattering of cholangiocarcinoma cells by disrupting adherens junctions. EGF-treated cholangiocarcinoma cells display internalization and decreased expression of E-cadherin, along with nuclear translocation of β-catenin [6].

EGF is a crucial growth factor that regulates cell survival [7]. EGF binds to the cell surface EGFR, activating downstream signal transduction. Through binding to the cell surface receptors, EGF activates an extensive network of signal transduction pathways, including activation of the phosphoinositide 3-kinase (PI3K)/AKT, rat sarcoma (RAS)/extracellular signal-regulated kinase 1/2 (ERK1/2), and janus kinase (JAK)/signal transducer and activator of transcription (STAT) pathways [8]. These pathways predominantly lead to the activation or inhibition of transcription factors that regulate the expression of both pro- and anti-apoptotic proteins, effectively blocking the apoptotic pathway [8]. In addition, the complex of ligands and receptors translocates to the nucleus to bind with the promoter and activate gene expression [9, 10]. In cancer, EGF signaling pathways are often dysfunctional, and targeted therapies that block EGF signaling have successfully treated cancers [6].

Checkpoint programmed cell death protein 1 (PD-1)/ PD-L1 plays a vital role in cancer proliferation, protecting tumor cells against immune demolition [11-13]. The expression of PD-L1 is regulated by the activity of the mitogen-activated protein kinase (MAPK) pathway [14]. The *KRAS* gene encodes a guanosine triphosphate (GTP)-binding protein and this KRAS protein plays a crucial role in the downstream survival-promoting regulatory signaling pathways connected to EGFR [15]. The mutation of *KRAS* leads to its constitutive activation. It triggers the activation of downstream signaling pathways, such as rapidly accelerated fibrosarcoma (RAF)/mitogen-activated protein kinase kinase (MEK)/ERK and PI3K/AKT/mammalian target of rapamycin (mTOR), which promote cell proliferation [16]. In patients receiving gefitinib treatment, AKT activation correlates with disease progression in wild-type EGFR lung adenocarcinoma. In *KRAS* mutant cells, administering insulin-like growth factor 1 receptor (IGF1R)-TKIs may attenuate AKT signaling and potentially restore sensitivity to gefitinib [17]. Gefitinib is a radiosensitizer that blocks radiation-triggered EGFR phosphorylation and subsequent downstream pathway activation. This action enhances the radiosensitivity of cholangiocarcinoma cells [5, 18]. Hence, identifying alternative compounds capable of inhibiting the cancer progression of *KRAS*-mutated cholangiocarcinoma cells is crucial.

Integrin αvβ3 plays an important role in signal transduction and downstream biological activities, including proliferation and migration in cancer cells. Targeting integrin αvβ3 has been shown highly interesting research issue in anti-cancer drug development. An integrin αvβ3 antagonist, heteronemin, inhibits cell proliferation by blocking EGF-induced PD-L1 expression through the transforming growth factor-β1 (TGF-β1)/ERK1/2 pathway. Heteronemin (Haimian jing) is a marine natural product extracted from *Hippospongia sp.*, a sesterterpenoid-type secondary metabolite found in marine sponges [19]. In the present report, we first investigated how EGFR

regulates cell proliferation via specific signal transduction pathways. Then, we explored whether and how heteronemin inhibits EGF-induced proliferation in cholangiocarcinoma cells. Finally, we showed that nano-tetrac derivative, DL-N2 can inhibit xenografted cholangiocarcinoma growth by inhibiting integrin αvβ3-depdent signal transduction pathways.

RESULTS

EGF induces signal transduction and cancer cell growth in cholangiocarcinoma cells.

EGF stimulates cancer growth via binding to its receptor, EGFR. However, it is still unclear whether EGF can promote the growth of cholangiocarcinoma cells. Here, we first examine the growth effect of activated EGFR on two cholangiocarcinoma cell lines, *KRAS* wild-type SSP-25 and *KRAS* mutant HuCCT1, by treating them with various concentrations of EGF (10, 20, 40, and 100 ng/ml).

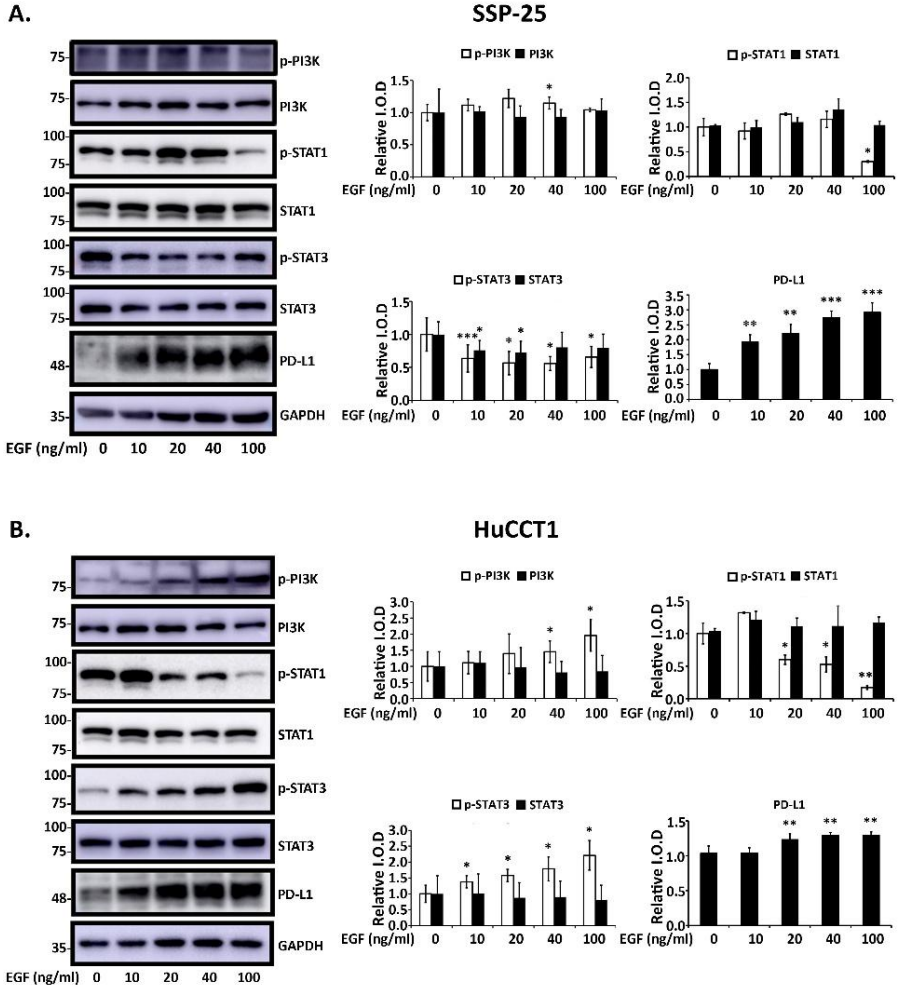

Figure 1. EGF modulates signal transduction pathways in cholangiocarcinoma cells. Serum-starved SSP-25 (A) and HuCCT1 cells (B) were left unstimulated or stimulated with various concentrations of EGF (10, 20, 40, and 100 ng/ml) for 24 h. The cells were then lysed, and cell lysates were subjected to Western blotting for the detection of p-PI3K, PI3K, p-STAT1, STAT1, p-STAT3, STAT3, PD-L1, and GAPDH, as a loading control for protein normalization. The quantitative results were expressed as relative integrated optical density (I.O.D.) by defining the amounts of the indicated detected proteins in unstimulated cells considered as 1. Data are represented as the mean ± SD of

three independent experiments. * P < 0.05, ** P < 0.01, and *** P < 0.001 compared to unstimulated cells.

In SSP-25 cells, EGF induced the phosphorylation of PI3K and STAT1 in the range of 10 to 40 ng/ml and 20 to 40 ng/ml, respectively **(Figure 1A)**. However, EGF inhibited STAT3 activation through suppression of STAT3 phosphorylation without affecting its protein level **(Figure 1A)**. Unlike its effect in SSP-25 cells, EGF stimulation of HuCCT1 cells increased the phosphorylation of PI3K and STAT3 in a concentration-dependent manner **(Figure 1B)**. EGF did not obviously alter STAT1 expression but significantly suppressed STAT1 phosphorylation **(Figure 1B)**. Additionally, EGF even at the lowest concentration stimulated the expression of PD-L1, a proliferation-related protein, in both cell lines **(Figure 1)**.

We also examined the effect of EGF on the proliferation of cholangiocarcinoma cells. SSP-25 cells and HuCCT1 were stimulated with different concentrations of EGF (10, 20, 40, and 100 ng/ml) for 72 h. EGF induced cell proliferation in SSP-25 cells starting at 20 ng/ml **(Figure 2A)**. Conversely, EGF only stimulated HuCCT1 cell proliferation at 100 ng/ml **(Figure 2B)**. Thus, EGF stimulation activates PI3K/STAT1 signaling to induce the proliferation of SSP-25 cells and PI3K/STAT3 signaling to induce the proliferation of HuCCT1 cells, respectively. To optimize the effect of heteronemin in both cell lines under EGF stimulation, we chose 100 ng/ml EGF for the following experiments.

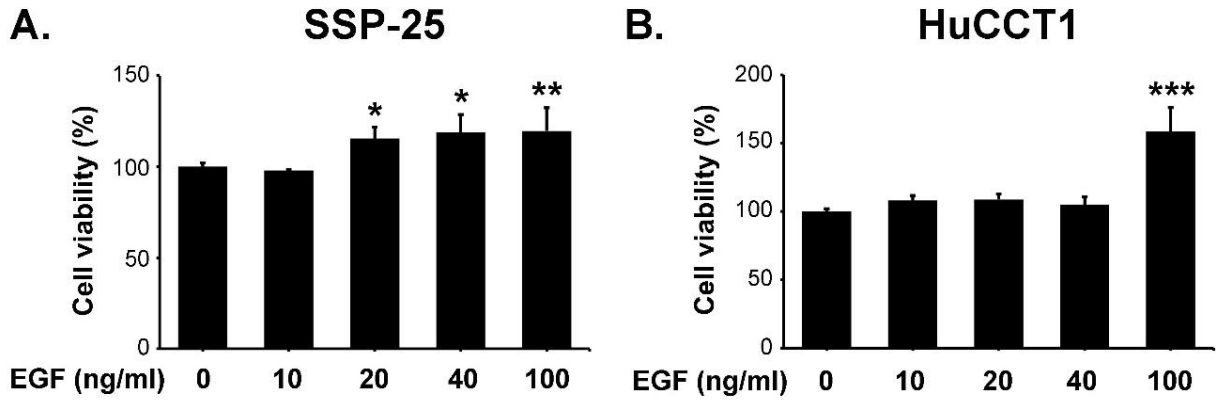

Figure 2. EGF stimulates the growth of cholangiocarcinoma cells. Serum-starved SSP-25 (A) and HuCCT1 cells (B) were left unstimulated or stimulated with various concentrations of EGF (10, 20, 40, and 100 ng/ml) for 72 h. The cells were then subjected to the CCK-8 cell proliferation assay. The quantitative results were expressed as a percentage (%) by defining the viability of the unstimulated group of each cell line as 100. Data are represented as the mean ± SD of triplicate cultures in three independent experiments. * P < 0.05, ** P < 0.01, and *** P < 0.001 compared to the unstimulated cells.

Integrin αvβ3 antagonist, heteronemin inhibited cell proliferation in cholangiocarcinoma cells by down-regulating the gene expression of proliferation-related genes.

Heteronemin has been shown to have anti-proliferative effects in various cancer cells, including cholangiocarcinoma [19-25]. However, the signal transduction pathways underlying how heteronemin causes this anti-proliferative effect in cholangiocarcinoma cells remain unknown. We first examined the growth inhibition effect of heteronemin in two different types of cholangiocarcinoma cells. SSP-25 and HuCCT1 cells were treated with various concentrations of

heteronemin for 72 h. Heteronemin caused a significant cytotoxic effect in both cell lines, starting at 0.3 μM, in a concentration-dependent manner **(Figure 3)**.

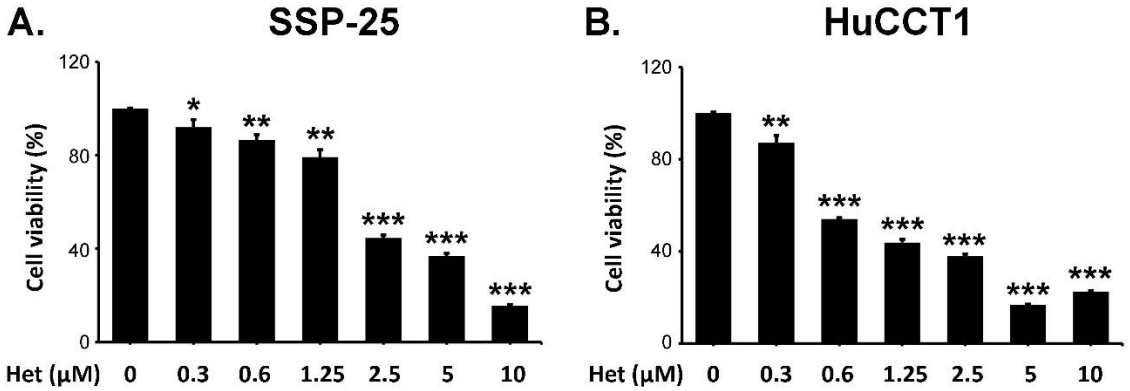

Figure 3. Heteronemin inhibits the growth of cholangiocarcinoma cells. Serum-starved SSP-25 (A) and HuCCT1 cells (B) were left untreated or treated with various concentrations of heteronemin (0.3, 0.6, 1.25, 2.5, 5, and 10 μM) for 72 h. The cells were then subjected to the CCK-8 cell proliferation assay. The quantitative results were expressed as a percentage (%) by defining the viability of the untreated group of each cell line as 100. Data are represented as the mean ± SD of triplicate cultures in four independent experiments. * $P < 0.05$, ** $P < 0.01$, and *** $P < 0.001$ compared to the untreated cells.

To further explore the suppressed growth effects of heteronemin on SSP-25 and HuCCT1 cells, particularly related to the differential expression of proliferation-related genes *PCNA*, *CCND1*, and *c-Myc*, SSP-25 and HuCCT1 cells were treated with the indicated concentrations of heteronemin for 24 h. In SSP-25 cells, heteronemin down-regulated the gene expression of *PCNA* and *CCND1* in a concentration-dependent manner **(Figure 4A)**. The expression of these two genes in HuCCT1 cells was suppressed by approximately 90% under heteronemin treatment within the range of 0.6 to 5 μM **(Figure 4B)**. However, in both SSP-25 and HuCCT1 cells, different concentrations of heteronemin showed contrasting effects on *c-Myc* expression. Lower concentrations (0.6 and 1.25 μM) of heteronemin exhibited an increase in effect. In contrast, higher concentrations (5 and 10 μM) inhibited this gene expression **(Figure 4)**. In addition, we also examined the effect of heteronemin on the expression of *EGFR* in both cell lines. Only 5 and 10 μM heteronemin inhibited *EGFR* expression in SSP-25 cells **(Figure 4A)**. However, it significantly suppressed *EGFR* expression in HuCCT1 cells even at the lowest concentration (0.3 μM) **(Figure 4B)**. These results indicated that heteronemin reduces the expression of proliferation-related genes *PCNA*, *CCND1*, *c-Myc*, and *EGFR* in both cholangiocarcinoma cell lines. Additionally, *KRAS* mutant HuCCT1 cells showed more sensitivity to heteronemin treatment.

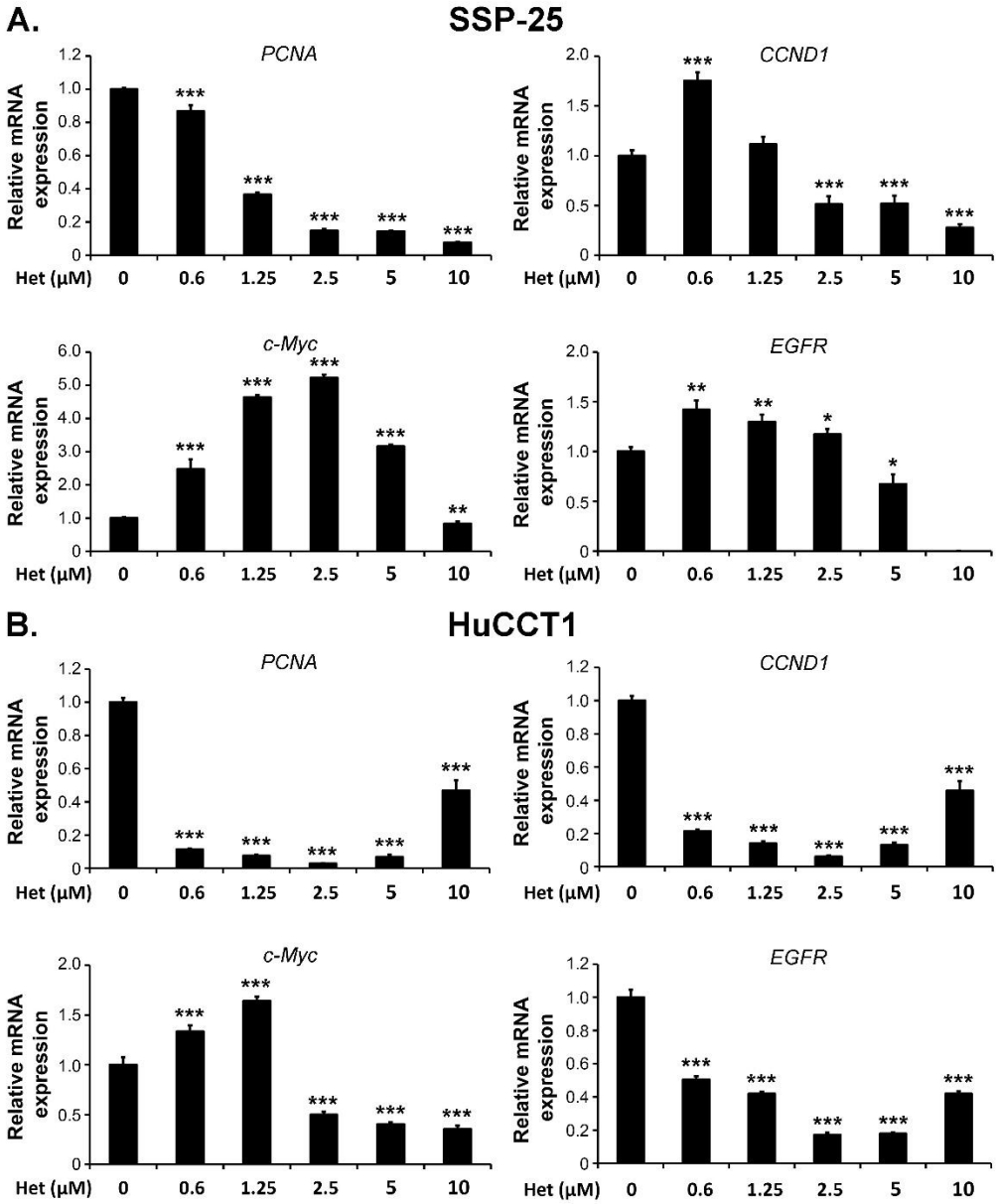

Figure 4. Heteronemin inhibits the expression of proliferation-related genes in cholangiocarcinoma cells. Serum-starved SSP-25 (A) and HuCCT1 cells (B) were left untreated or treated with various concentrations of heteronemin (0.3, 0.6, 1.25, 2.5, 5, and 10 μM) for 24 h. The cells were lysed, and the mRNAs extracted from cell lysates were subjected to the reverse transcription reaction. The mRNA expression of *PCNA*, *CCND1*, *c-Myc*, *EGFR*, and *18S rRNA*, as a loading control, was quantified by qRT-PCR. The mRNA expression of these genes was normalized to that of *18S rRNA*. The quantitative values were expressed as relative mRNA levels by defining the amounts of gene expression in the untreated group of each cell line as 1. Data are represented as the mean ± SD of quadruplicate wells in three independent experiments. * $P < 0.05$, ** $P < 0.01$, and *** $P < 0.001$ compared to the untreated cells.

Interference with integrin αvβ3 activities alters EGF-induced signal transduction in cholangiocarcinoma.

The activated EGFR signal transduction pathway induces cellular motility [26] and promotes cancer cell growth [6, 7]. Recently, we have shown that heteronemin inhibits the EGFR signal transduction pathway to down-regulate the proliferation of colorectal cancer cells [21]. To further investigate whether heteronemin suppresses the signal transduction pathways activated by EGF in cholangiocarcinoma cells, SSP-25 and HuCCT1 cells were stimulated with 100 ng/ml EGF in the presence or absence of the indicated concentrations of heteronemin for 24 h. In SSP-25 cells, PI3K and its phosphorylated forms increased in heteronemin-treated cells in a concentration-dependent manner up to 1.25 μM (**Figure 5**). After treatment with 1.25 and 2.5 μM heteronemin in this cell, the phosphorylation of STAT1 showed a significant increase compared to untreated cells. In contrast to the phosphorylation of PI3K, the phosphorylation pattern of STAT3 decreased in heteronemin-treated cells in a concentration-dependent manner. Heteronemin inhibited the EGF-induced phosphorylation of PI3K in SSP-25 cells (**Figure 5**). The phosphorylation of both STAT1 and STAT3 increased in a concentration-dependent manner under the treatment of heteronemin in EGF-stimulated cells, except for the effect of 2.5 μM heteronemin on STAT3.

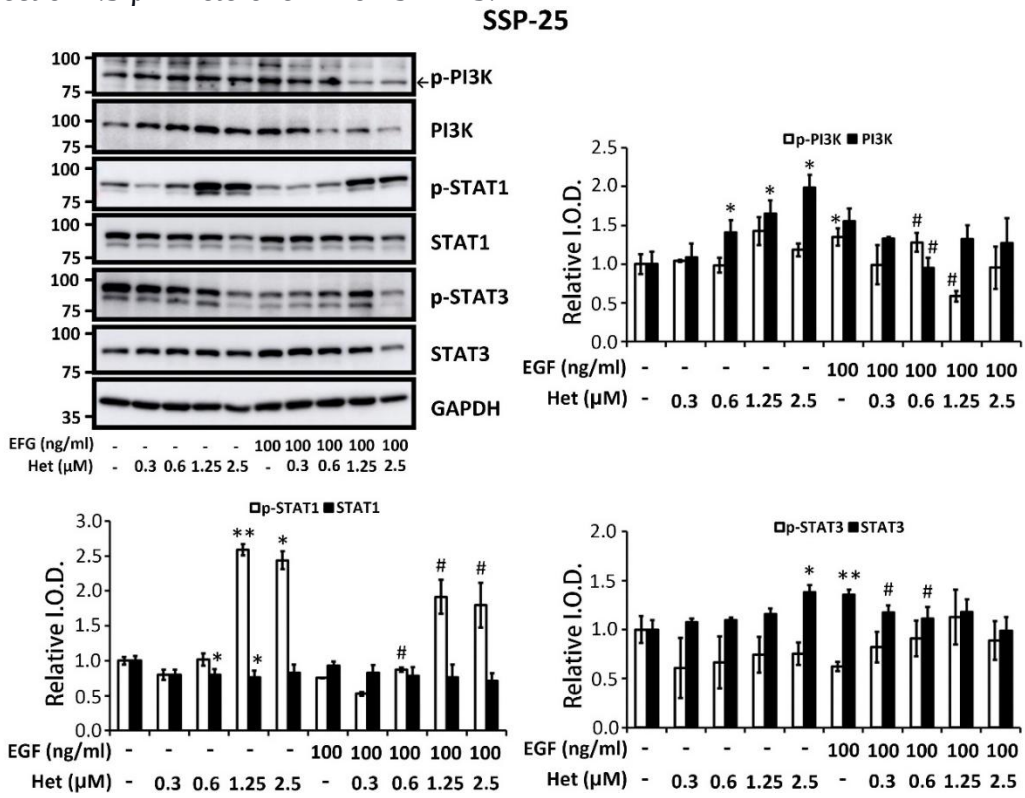

Figure 5. Heteronemin affects EGF-induced PI3K, STAT1, and STAT3 activation in cholangiocarcinoma SSP-25 cells. Serum-starved SSP-25 cells were left untreated or treated with various concentrations of heteronemin (0.3, 0.6, 1.25, and 2.5 μM) together with or without 100 ng/ml EGF for 24 h. The cells were then lysed, and cell lysates were subjected to Western blotting for the detection of p-PI3K, PI3K, p-STAT1, STAT1, p-STAT3, STAT3, and GAPDH as a loading control for protein normalization. The quantitative results were expressed as relative I.O.D. by defining the amounts of the indicated detected proteins in unstimulated cells, with the absence of heteronemin treatment considered as 1. Data are represented as the mean ± SD of three independent experiments. * $P < 0.05$ and ** $P < 0.01$ compared to untreated cells, where the absence of heteronemin treatment. # $P < 0.05$ compared to EGF-stimulated cells, where the absence of heteronemin treatment.

A parallel experiment was conducted in HuCCT-1 cells, wherein heteronemin suppressed EGF-induced signal transduction pathways. Heteronemin induced the phosphorylation of PI3K, STAT1, and STAT3 up to 1.25 μM in HuCCT-1 cells (**Figure 6**). On the other hand, 100 ng/ml EGF increased PI3K, STAT1, and STAT3, as well as their phosphorylated forms, compared to unstimulated cells. Heteronemin inhibited the EGF-induced phosphorylation of PI3K, STAT1, and STAT3 in a concentration-dependent manner (**Figure 6**). In addition, the levels of PI3K, STAT1, and STAT3 decreased under treatment with 2.5 μM heteronemin in HuCCT1 cells. These results indicate that heteronemin inhibits the proliferation of SSP-25 and HuCCT1 cells by suppressing different signaling pathways induced by EGF.

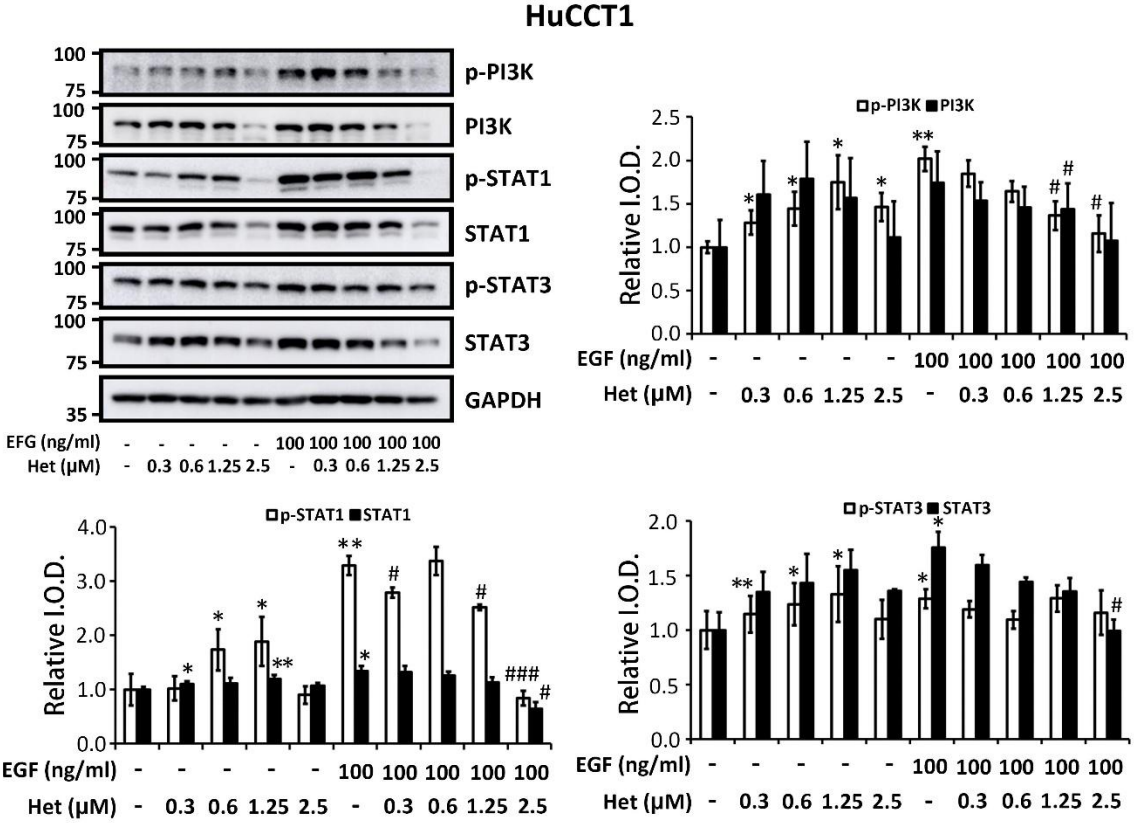

Figure 6. Heteronemin affects EGF-induced activation of PI3K, STAT1, and STAT3 in cholangiocarcinoma HuCCT1 cells. Serum-starved HuCCT1 cells were left untreated or treated with various concentrations of heteronemin (0.3, 0.6, 1.25, and 2.5 μM) together with or without 100 ng/ml EGF for 24 h. The cells were then lysed, and cell lysates were subjected to Western blotting for the detection of p-PI3K, PI3K, p-STAT1, STAT1, p-STAT3, STAT3, and GAPDH as a loading control for protein normalization. The quantitative results were expressed as relative I.O.D. by defining the amounts of the indicated detected proteins in unstimulated cells, with the absence of heteronemin treatment considered as 1. Data are represented as the mean ± SD of three independent experiments. * $P < 0.05$ and ** $P < 0.01$ compared to untreated cells, where the absence of heteronemin treatment. # $P < 0.05$ compared to EGF-stimulated cells, where the absence of heteronemin treatment.

Interference with integrin αvβ3 activities inhibits EGF-induced PD-L1 expression and cell proliferation in cholangiocarcinoma cells.

As shown in Figure 1 and 2, PI3K may play a crucial role in promoting EGF-triggered proliferation in cholangiocarcinoma cells. Moreover, EGF led to a concentration-dependent elevation in PD-L1 expression, as depicted in Figure 1. Notably, heteronemin was observed to suppress EGF-induced PI3K activation (**Figure**s **5** and **6**). To determine whether heteronemin inhibits the proliferation of cholangiocarcinoma cells via the PI3K signaling transduction pathway activated by EGF, the expression of PD-L1 in SSP-25 and HuCCT1 cells was examined by stimulating them with 100 ng/ml of EGF in the presence of different concentrations of heteronemin for 24 h. Heteronemin treatment increased PD-L1 expression in SSP-25 cells. It decreased PD-L1 expression in HuCCT1 cells in a concentration-dependent manner (**Figure 7**). EGF-induced PD-L1 expression in both cholangiocarcinoma cell lines, and this effect was concentration-dependently inhibited by heteronemin (**Figure 7**).

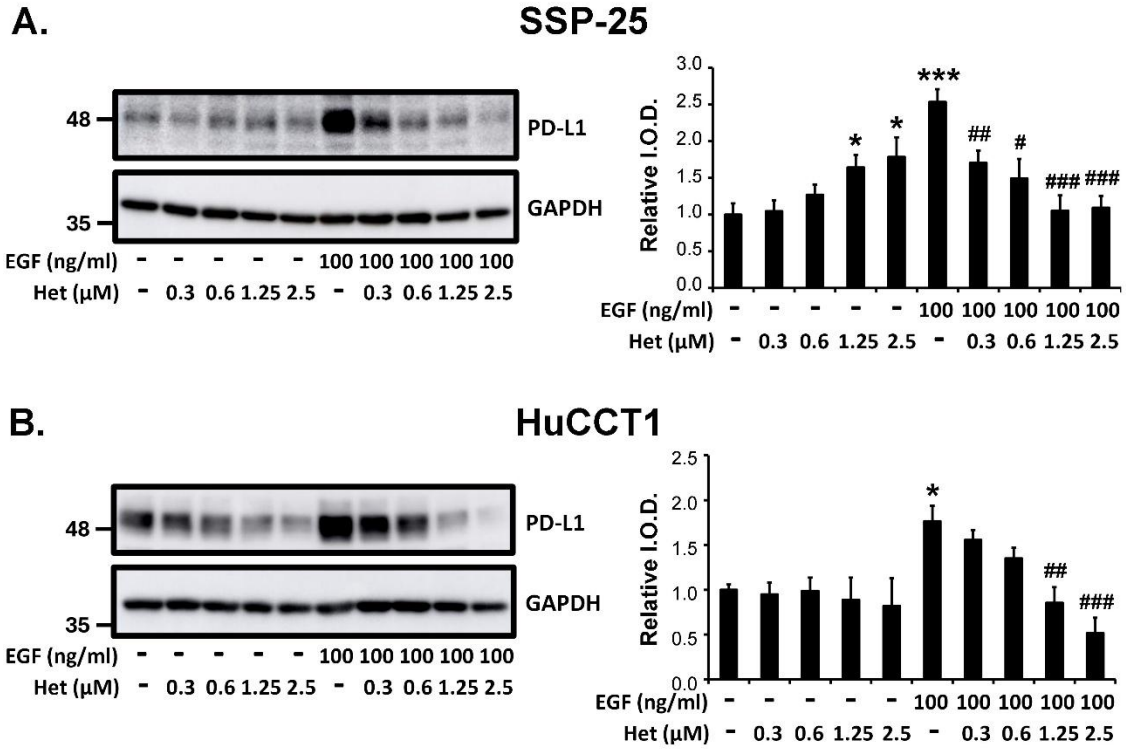

Figure 7. Heteronemin blocks EGF-induced PD-L1 expression in cholangiocarcinoma cells. Serum-starved SSP-25 (A) and HuCCT1 cells (B) were left untreated or treated with various concentrations of heteronemin (0.3, 0.6, 1.25, and 2.5 μM) together with or without 100 ng/ml EGF for 24 h. The cells were then lysed, and cell lysates were subjected to Western blotting to detect PD-L1 and GAPDH as a loading control for protein normalization. The quantitative results were expressed as relative I.O.D. by defining the amounts of PD-L1 in untreated cells, with the absence of heteronemin treatment considered 1. Data are represented as the mean ± SD of three independent experiments. * $P < 0.05$ and *** $P < 0.001$ compared to untreated cells, where the absence of heteronemin treatment. # $P < 0.05$, ## $P < 0.01$, and ### $P < 0.001$ compared to EGF-stimulated cells, where the absence of heteronemin treatment.

We next investigated the role of PI3K in the heteronemin-induced inhibitory effect on EGF-induced proliferation in cholangiocarcinoma cells. Two cholangiocarcinoma cell lines were treated with EGF and heteronemin, either alone or in the presence of a specific PI3K inhibitor, LY294002, for 72 h. In both cell lines, the PI3K inhibitor LY294002 not only suppressed cell proliferation on its own but also inhibited EGF-induced cancer cell growth (**Figure 8**). Heteronemin similarly inhibited cancer cell growth in both control and EGF-stimulated cells. However, the combined treatment of heteronemin and LY294002 did not further affect cell viability (**Figure 8**). Thus, the inhibitory effect of heteronemin on EGF-induced cell proliferation depends on the suppression of PI3K activity.

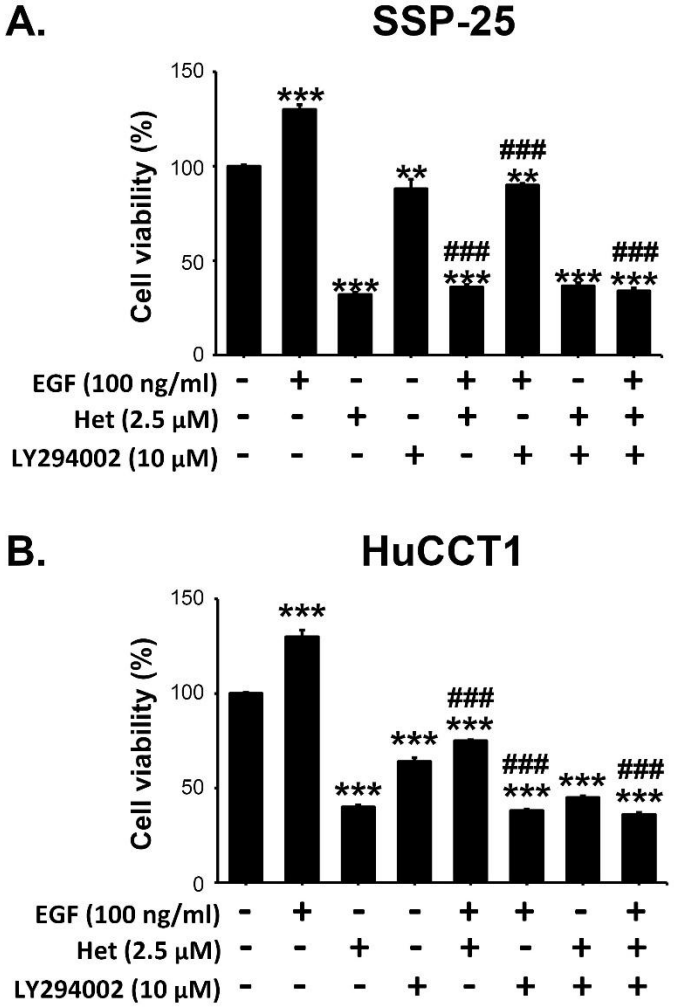

Figure 8. Heteronemin suppresses PI3K signaling to inhibit cell proliferation in EGF-stimulated cholangiocarcinoma cells. Serum-starved SSP-25 (A) and HuCCT1 cells (B) were left unpretreated or pretreated with 10 μM LY294002 and then left untreated or treated with 2.5 μM heteronemin together with or without 100 ng/ml EGF for 72 h. The cells were then subjected to the CCK-8 cell proliferation assay. The quantitative results were expressed as a percentage (%) by defining the viability of untreated cells as 100. Data are represented as the mean ± SD of triplicate cultures in four independent experiments. ** $P < 0.01$ and *** $P < 0.001$ compared to EGF-unstimulated cells, in which LY294002 or heteronemin treatment was absent. ### $P < 0.001$ compared to EGF-stimulated cells, where the absence of LY294002 or heteronemin treatment.

DL-N2 and DL-N2-Dox inhibit tumor size in xenografted mice.

We have developed a novel nano-tetrac integrin αvβ3 antagonist (DL-N2). To examine the efficacy of DL-N2, Lipo-Doxorubicin or DL-N2 payload Doxorubicin, mice were treated with either DL-N2 (tetrac 0.1 mg/kg), Lipo-Dox (Dox 2mg/kg), or DL-N2-Dox (tetrac 0.1 mg/kg, Dox 2mg/kg) twice a week for five weeks. Tumor sizes were measured at the date indicated. The tumor growth rate in the control group mice grew consistently shown in **Figure 9**. Lipo-Dox (Dox 2mg/kg) inhibited tumor growth. DL-N2 and DL-N2-Dox significantly suppressed tumor growth rates in the first week after treatment (**Figure 9**). The inhibitory effects maintained constant significantly until the five-week treatment (**Figure 9**). In addition, the harvested tumor sizes from DL-N2 and DL-N2-Dox treated mice were smaller than Lipo-Dox-treated mice generally (**Results not shown**).

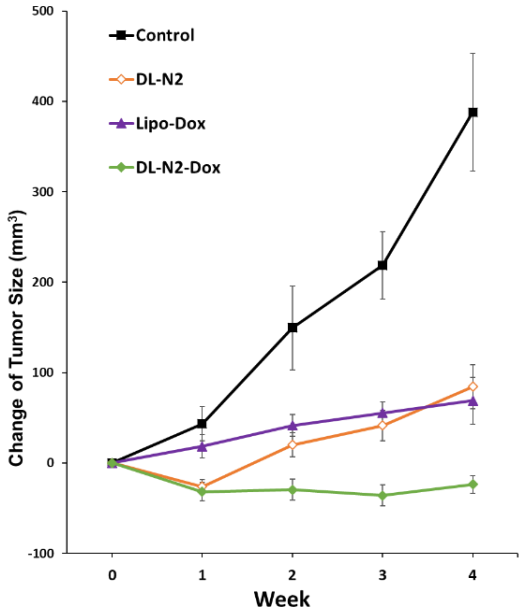

Figure 9. DL-N2 and DL-N2-Dox show a better effect to reduce the tumor size in TFK-1 xenograft study. After TFK-1cancer cell inoculation in the Balb c/ nude mice, the mice were treated with solvent (PBS), DL-N2 (tetrac, 0.1 mg/kg), Lipo-Dox (Dox, 2 mg/kg) or DL-N2-Dox (tetrac, 0.1 mg/kg, Dox, 2 mg/kg) for 5 weeks. Tumor sizes of DL-N2 or DL-N2-Dox-treated mice were smaller than those of the control group and lipo-Dox-treated group. After TFK-1 cell inoculation, the mice were treated intraperitoneally with solvent (PBS), DL-N2, Lipo-Dox, or DL-N2payloadDox for five weeks.

DISCUSSION

In order to seek the proper anti-cholangiocarcinoma therapies, we investigated the possibility of targeting EGF-stimulated cancer growth via targeting integrin αvβ3. Our study shows that EGF stimulates the growth of cholangiocarcinoma *KRAS* wild-type SSP-25 and *KRAS* mutant HuCCT1 cells at 20 ng/ml and 100 ng/ml, respectively. PI3K is identified as a critical kinase-inducing cell growth activated by EGF in these two cell lines. Additionally, ERK1/2 activation is observed under EGF stimulation (Data not shown). Integrin αvβ3 antagonist heteronemin suppresses EGF-stimulated cell growth through different signaling pathways. In SSP-25 cells, it activates the PI3K/STAT3/PD-L1 pathway, whereas in HuCCT1 cells, it induces the PI3K/STAT1/PD-L1 pathway.

Combining heteronemin with other compounds can enhance the inhibitory effect on EGF-mediated *KRAS* mutant cancer progression. In *KRAS* mutant colon cancer HCT-116 cells, heteronemin and tetraiodothyroacetic acid (tetrac), a derivative of thyroid hormone, and their combined treatment induce an antiproliferative effect[21]. Mutant *KRAS* notably contributes to the therapeutic resistance observed in cholangiocarcinoma patients. Heteronemin reduced the EGF-induced proliferation of *KRAS* mutant cholangiocarcinoma HuCCT1 cells (**Figure 3**). Combining heteronemin with tetrac reduced the expression levels of signal transduction pathways involved in EGFR signaling, including those related to cell proliferation, angiogenesis, and EMT in tumor metastasis, compared to heteronemin alone. Conversely, cell motility exhibited an inverse expression pattern across all signal transduction pathways driving cancer progression. Inhibiting cell surface PD-L1 with a specific antibody led to a notable decrease in tumorsphere formation. However, it did not hinder sphere growth, indicating that cell surface PD-L1 might be an adhesive molecule for colon and breast cancer stem cells[27]. Nevertheless, only cell motility exhibited an inverse correlation among pathway scores of the EGFR following heteronemin or combination treatment[21]. Cancers with *KRAS* mutations always display high mortality due to the ineffective function of therapeutic drugs. Thus, heteronemin combined with other potential compounds such as tetrac could be a new approach to treating *KRAS* mutant cancer. Targeting integrin αvβ3 by heteronemin and tetrac derivatives inhibits cancer cell growth. Studies in cholangiocarcinoma xenograft indicated that tetrac derivative, DL-N2, and DL-N2 payload doxorubicin showed better anti-cancer growth in xenograft (**Figure 9**).

Our data and the previous findings support the idea that combining EGFR inhibitors and heteronemin could be a new therapeutic approach for inhibiting the proliferation or metastasis of cholangiocarcinoma cells. Additionally, tetrac derivatives such as DL-N2 can be used to payload other anti-cancer materials such as doxorubicin and Heteronemin to construct a more effective, less toxic, multiple-target combination therapeutic agent for cholangiocarcinoma. Our idea of DL-N2 payloads can be used for future integrated grant applications.

MATERIAL and METHODS

Cell cultures

Two human cholangiocarcinoma cell lines, *KRAS* wild-type SSP-25 and *KRAS* mutant HuCCT1, were obtained from Riken Bioresource Research Center (Tsukuba, Japan). Cells were cultured in RPMI-1640 medium supplemented with 10% fetal bovine serum in a humidified incubator with 5% CO_2 at 37ºC. For serum starvation, cells were placed in a 0.25% hormone-depleted serum-supplemented medium for 2 days.

Quantitative reverse transcription polymerase chain reaction (qRT-PCR)

SSP-25 and HuCCT1 cells were seeded at a density of 2×10^5 cells/well in 6-well plates. After seeding, the medium was replaced with a 0.25% hormone-depleted serum-supplemented medium for 48 h. Serum-starved cells were treated with various concentrations of heteronemin (0.6, 1.25, 2.5, 5, and 10 μM) for 24 h in a 5% hormone-depleted serum-supplemented medium. Total RNA was extracted, and genomic DNA was removed with an Illustra RNAspin Mini RNA Isolation Kit (GE Healthcare Life Sciences, Buckinghamshire, UK). Deoxyribonuclease I (DNase I)-treated total RNA (1 μg) was reverse-transcribed using a RevertAid H Minus First Strand complementary DNA (cDNA) Synthesis Kit (Life Technologies) into cDNA. cDNAs were used as the template for the real-time PCR analysis. Real-time PCRs were conducted using a QuantiNovaTM SYBR® Green PCR Kit (Qiagen, Hilden, Germany) on a CFX Connect™ Real-Time PCR Detection System (Bio-Rad Laboratories, Hercules, CA, USA). Primer sequences were as follows: Homo sapiens cyclin D1 (CCND1), forward 5'-CAA GGC CTG AAC CTG AGG AG-3' and reverse 5'-GAT CAC TCT GGA GAG GAA GCG-3' (Accession No.: NM_053056); Homo sapiens proliferating cell nuclear antigen

(PCNA), forward 5'-TCTGAGGGCTTCGACACCTA-3' and reverse 5'-TCA TTG CCG GCG CAT TTT AG-3' (Accession No.: BC062439.1); Homo sapiens cytosol MYC proto-oncogene, bHLH transcription factor (c-Myc), forward 5'-TTCGGGTAGTGGAAAACCAG-3' and reverse 5'-CAGCAGCTCGAATTTCTTCC -3' (Accession No. NM_002467.4); Homo sapiens EGFR, forward 5'- AATTTACAGGAAATCCTGCATGGC-3' and reverse 5'- GATGCTCTCCACGTTGCACA-3' (Accession No. NM_005228); Homo sapiens 18S ribosomal RNA (18S rRNA), forward 5'-GTAACCCGTTGAACCCCATT-3' and reverse 5'- CCATCCAATCGGTAGTAGCG-3' (Accession No. NR_003286.2). Calculations of relative gene expressions (normalized to the 18S rRNA reference gene) were performed according to the ΔΔCT method. The fidelity of the PCR was determined with a melting temperature analysis.

Western blotting

To examine signal transduction pathways involved in EGF-induced PD-L1 expression and effects of heteronemin on EGF-induced PD-L1 expression in SSP-25 and HuCCT1 cells, western blot analysis was performed to detect the protein expression levels of PD-L1 and the activation of PI3K, STAT1, and STAT3 in the total cell lysates of cells that had been treated with vehicle for 24 h. Protein samples were resolved on a 10% sodium dodecyl-sulfate polyacrylamide gel electrophoresis (SDS-PAGE). A 20-μg quantity of protein was loaded in each well with sample buffer, and the samples were resolved with electrophoresis at 100 V for 2 h. The resolved proteins were transferred from the polyacrylamide gel to Millipore Immobilon-PSQ Transfer polyvinylidene fluoride (PVDF) membranes (Millipore, Billerica, MA) with the Mini Trans-Blot® Cell (Bio-Rad Laboratories, Inc.). Membranes were blocked with a solution of 2% bovine serum albumin in Tris-buffered saline (TBS) with 0.1% tween-20 (TBST) and incubated with primary antibodies to PD-L1 (Cat. No.: GTX104763, GeneTex International Corp., Hsinchu City, Taiwan) at a dilution factor of 1:1000, PI3K (Cat. No.: 610046, BD Biosciences, San Diego, CA, USA) at a dilution factor of 1:1000, p-PI3K p85 (Tyr458)/p55 (Tyr199) (Cat. No.: 4228, Cell Signaling Technology, Beverly, MA, USA) at a dilution factor of 1:3000, STAT1 (Cat. No.: 66545-1-1g, Proteintech, Rosemont, IL, USA) at a dilution factor of 1:1000, p-STAT1 (Tyr701) (Cat. No.: 9167, Cell Signaling Technology, Beverly, MA, USA) at a dilution factor of 1:1000, STAT3 (Cat. No.: 610190, BD Biosciences, San Diego, CA, USA) at a dilution factor of 1:1000, p-STAT3 (Tyr705) (Cat. No.: 9145, Cell Signaling Technology, Beverly, MA, USA) at a dilution factor of 1:1000, and glyceraldehyde-3-phosphate dehydrogenase (GAPDH) (Cat. No.: 60004-1, GeneTex International Corp., Hsinchu City, Taiwan) at a dilution factor of 1:20000 at 4ºC overnight. The antibody-probed membrane was washed with TBST containing 5% fat-free milk (5% TBST/milk) three times for 10 min and then probed with goat anti-mouse immunoglobulin G (IgG) (Cat. No.: GTX213111-05, GeneTex International Corp., Hsinchu City, Taiwan) or goat anti-rabbit IgG (Cat. No.: GTX213110-04, GeneTex International Corp., Hsinchu City, Taiwan) horseradish peroxidase (HRP)-conjugated secondary antibodies, which were prepared in 5% TBST/milk at a dilution of 1:20000, at room temperature for 1 h. After the membrane was washed three times for 10 min by TBS, chemiluminescent detection was performed using Immobilon Western Chemiluminescent HRP Substrate (Millipore, Billerica, MA). The bands were imaged by BioSpectrum Imaging System (UVP, LLC, Upland, CA, USA) and quantified using densitometry by Image J 1.47 software (National Institute of Health, USA) according to the software instruction.

Cell viability assay

SSP-25 and HuCCT1 cells were seeded in 96-well plates at a density of 3000 cells/well. After 24 h of cell attachment, cells were starved with 0.25% hormone-depleted serum-supplemented medium for 48 h. Then, serum-starved cells were treated with various concentrations of EGF and heteronemin or 10 μM LY294002 in a 5% hormone-depleted serum-supplemented medium for 72 h.

Medium and reagents were refreshed daily. Cell proliferation was assayed using the Cell Counting Kit-8 (CCK-8) (Cat. No.: 96992, Sigma-Aldrich, St. Louis, MO, USA), according to the manufacturer's instructions.

Statistical analysis

In this study, the statistical significance of all other data was analyzed by a two-tailed Student's t-test using Excel 2010. All data are presented as mean ± standard deviation (SD). $P < 0.05$ (* or #), $P < 0.01$ (** or ##), and $P < 0.001$ (*** or ###) are considered as statistically significant.

REFERENCES

1. Sarcognato, S., et al., *Cholangiocarcinoma.* Pathologica, 2021. **113**(3): p. 158-169.
2. Hsu, M., et al., *KRAS and GNAS mutations and p53 overexpression in biliary intraepithelial neoplasia and intrahepatic cholangiocarcinomas.* Cancer, 2013. **119**(9): p. 1669-74.
3. Wu, C.C., et al., *Aurora-A promotes gefitinib resistance via a NF-κB signaling pathway in p53 knockdown lung cancer cells.* Biochem Biophys Res Commun, 2011. **405**(2): p. 168-72.
4. Massarelli, E., et al., *KRAS mutation is an important predictor of resistance to therapy with epidermal growth factor receptor tyrosine kinase inhibitors in non-small-cell lung cancer.* Clin Cancer Res, 2007. **13**(10): p. 2890-6.
5. Leone, F., et al., *Somatic mutations of epidermal growth factor receptor in bile duct and gallbladder carcinoma.* Clin Cancer Res, 2006. **12**(6): p. 1680-5.
6. Clapéron, A., et al., *EGF/EGFR axis contributes to the progression of cholangiocarcinoma through the induction of an epithelial-mesenchymal transition.* J Hepatol, 2014. **61**(2): p. 325-32.
7. Henson, E.S. and S.B. Gibson, *Surviving cell death through epidermal growth factor (EGF) signal transduction pathways: implications for cancer therapy.* Cell Signal, 2006. **18**(12): p. 2089-97.
8. Normanno, N., et al., *Epidermal growth factor receptor (EGFR) signaling in cancer.* Gene, 2006. **366**(1): p. 2-16.
9. Wieduwilt, M.J. and M.M. Moasser, *The epidermal growth factor receptor family: biology driving targeted therapeutics.* Cell Mol Life Sci, 2008. **65**(10): p. 1566-84.
10. Brand, T.M., et al., *The nuclear epidermal growth factor receptor signaling network and its role in cancer.* Discov Med, 2011. **12**(66): p. 419-32.
11. Huang, T.Y., et al., *NDAT Targets PI3K-Mediated PD-L1 Upregulation to Reduce Proliferation in Gefitinib-Resistant Colorectal Cancer.* Cells, 2020. **9**(8).
12. Chen, L. and X. Han, *Anti-PD-1/PD-L1 therapy of human cancer: past, present, and future.* J Clin Invest, 2015. **125**(9): p. 3384-91.
13. Schmidt, L.H., et al., *PD-1 and PD-L1 Expression in NSCLC Indicate a Favorable Prognosis in Defined Subgroups.* PLoS One, 2015. **10**(8): p. e0136023.
14. Stutvoet, T.S., et al., *MAPK pathway activity plays a key role in PD-L1 expression of lung adenocarcinoma cells.* J Pathol, 2019. **249**(1): p. 52-64.
15. Schubbert, S., K. Shannon, and G. Bollag, *Hyperactive Ras in developmental disorders and cancer.* Nat Rev Cancer, 2007. **7**(4): p. 295-308.
16. Serna-Blasco, R., et al., *KRAS p.G12C mutation occurs in 1% of EGFR-mutated advanced non-small-cell lung cancer patients progressing on a first-line treatment with a tyrosine kinase inhibitor.* ESMO Open, 2021. **6**(5): p. 100279.
17. Jeannot, V., et al., *The PI3K/AKT pathway promotes gefitinib resistance in mutant KRAS lung adenocarcinoma by a deacetylase-dependent mechanism.* Int J Cancer, 2014. **134**(11): p. 2560-71.
18. Silini, A., et al., *Regulator of G-protein signaling 5 (RGS5) protein: a novel marker of cancer vasculature elicited and sustained by the tumor's proangiogenic microenvironment.* Cell Mol Life Sci, 2012. **69**(7): p. 1167-78.

19. Wang, K., et al., *The power of heteronemin in cancers.* J Biomed Sci, 2022. **29**(1): p. 41.
20. Lin, H.Y., et al., *Heteronemin Induces Anti-Proliferation in Cholangiocarcinoma Cells via Inhibiting TGF-β Pathway.* Mar Drugs, 2018. **16**(12).
21. Unson, S., et al., *Heteronemin and Tetrac Induce Anti-Proliferation by Blocking EGFR-Mediated Signaling in Colorectal Cancer Cells.* Mar Drugs, 2022. **20**(8).
22. Yang, Y.S.H., et al., *Effect of Estrogen on Heteronemin-Induced Anti-proliferative Effect in Breast Cancer Cells With Different Estrogen Receptor Status.* Front Cell Dev Biol, 2021. **9**: p. 688607.
23. Huang, C.H., et al., *Combined Treatment of Heteronemin and Tetrac Induces Antiproliferation in Oral Cancer Cells.* Mar Drugs, 2020. **18**(7).
24. Chung, C.C., et al., *Heteronemin and tetrac derivatives suppress non-small cell lung cancer growth via ERK1/2 inhibition.* Food Chem Toxicol, 2022. **161**: p. 112850.
25. Chang, W.T., et al., *A Marine Terpenoid, Heteronemin, Induces Both the Apoptosis and Ferroptosis of Hepatocellular Carcinoma Cells and Involves the ROS and MAPK Pathways.* Oxid Med Cell Longev, 2021. **2021**: p. 7689045.
26. Garcia, R., R.A. Franklin, and J.A. McCubrey, *EGF induces cell motility and multi-drug resistance gene expression in breast cancer cells.* Cell Cycle, 2006. **5**(23): p. 2820-6.
27. Chen, M., et al., *Insluin and epithelial growth factor (EGF) promote programmed death ligand 1(PD-L1) production and transport in colon cancer stem cells.* BMC Cancer, 2019. **19**(1): p. 153.

International Conference Attendance Report by Hung-Yun Lin, PhD

1. Attendance of AACR special conference in Boston

AACR Special Conference in Cancer Research: Translating Cancer Evolution and Data Science: The Next Frontier was held from 3rd to 6th December 2023 at Westin Copley Place, Boston, MA, USA. With session topics ranging from understanding the impact of cancer evolution on clinical research to decoding the evolutionary history of human tumors, this conference offers a unique platform for cancer researchers, oncologists, and data scientists to delve into a cross-disciplinary exploration of cancer evolution and its implications for diagnosis, treatment, and drug discovery. Many of the world's top scholars participated in the conference, and many new research breakthroughs and results were also published. In addition, many biotechnology manufacturers were exhibiting at the venue. The latest experimental testing instruments or reagents. The conference topics cover many fields of cancer treatment research, including molecular/cell biology genetics, bioinformatics and systems biology, tumor biology, cancer chemistry, clinical research, endocrinology, epidemiology, experiment and molecular therapeutics, immunology and preventive medicine research, etc. The annual conference of AACR brings together many cancer research experts worldwide, so there will be many seminar topics going on simultaneously. I only participate in topics that interest me.

On the first day of the seminar (Dec 03), the local temperature in Boston was relatively fair, close to 45 F. However, in the morning, participating scholars from around the world entered the venue one after another and went through the registration process. After a period of waiting, it was finally completed. Check-in and get your identification card. The seminar started at 8 a.m. after a grand opening ceremony and the organizer's speech. The first to appear are the Educational Sessions and Methods Workshops in many research fields, providing a basic introduction to participants not in this field. I participated in one of the symposiums with the theme "Theoretical Approaches to Fundamental Issues in Cancer." During the symposium, many well-known scholars presented their years of research experience, shared with everyone, and discussed the future research trends in cancer treatment. I participated in the OPENING PLENARY SESSION with the "Opening Plenary: Advancing Cancer Medicine: From Discovery to Patient Care" theme. The speaker shared various strategies, from developing new drugs to treating patients—psychological journey, for example, Immune checkpoint therapy from CTLA-4 to PD-1/PD-L1 and beyond etc. Because our laboratory is also developing new anti-cancer drugs targeting PD-L1, we can learn from others' successful experiences and possible problems and solutions to make the future research and development process smoother. On 04/12, I participated in the Major Symposium with the theme "Dharma Master Jiantai Symposium in Biomarkers: Insights into Tumor Cell Fates and Drug Resistance from Single-Cell Analyses." In recent years, the field of cancer treatment has made significant progress in the so-called Precision medicine, which is increasingly valued. The speakers shared their own research experiences and results, using single-cell analysis to discover the unique molecular profiles of cancer cells. Our post-presentation entitled Role of integrin αvβ3 in actions of steroid hormones in breast cancer was from 5:45 to 7:15 p.m. on Dec 05. Poster During the exhibition, scholars showed interest in our research and reports. During the Q&A process, I exchanged comments and suggestions for improving research methods

with scholars, which greatly benefited us. I attended small penal meetings and speeches on the last day (06 Dec). The theme centered on discussing the microenvironment of cancer cells and immune cells and was supported by clinical case statistics reports. The meeting ended perfectly with the applause of the scholars.

2. Accomplishment in attending the meeting

During these days of speeches and poster presentations, many new results and trends in cancer treatment were obtained. I have gained many insights into the current applications of cancer treatment worldwide. Further understanding is gained as to how far research into treatment has progressed. Various new therapies and discoveries in cancer treatment were reported, and the world's top scholars exchanged opinions at the conference. Although many advances still need further evaluation and revision, it also injected a new wave of enthusiasm into subsequent research directions. Our presentation revealed that molecular docking studies indicate the binding domain of the Asp (D) residue of the cRGD ligand plays a pivotal role in interactions between hormones and the heterodimeric integrin αvβ3. In addition, steroid hormones preferentially dock to the lower area of the cRGD site. These results are consistent with previous findings. The thyroid hormone pocket is near the top of the cRGD recognition site, and the steroid hormone pocket is at the bottom of the cRGD domain. Conveying a greater understanding of the intermolecular interactions can help design specific integrin αvβ3 inhibitors for therapeutic applications. Non-genomic downstream integrin αvβ3 signaling regulates nuclear transcription through different pathways, including classical nuclear receptor localization and changes in the phosphorylation of key nuclear signaling molecules. Understanding how genomic and non-genomic signaling work together to regulate critical biological processes can help better design the regulation of these processes. It also can improve the possibility of treating hormone-dependent breast cancer and other tumors such as prostate cancer and lung cancer.

Role of integrin αvβ3 in actions of steroid hormones in breast cancer

Chung-Che Tsai*, Zi-Lin Li*, Yi-Chen Chen, Tin-Yi Chu, Ju-Ku Mo, Ya-Jung Shih, Hung-Yun Lin, Kuan Wang

Graduate Institute of Cancer Biology and Drug Discovery, College of Medical Science and Technology, TMU Research Center of Cancer Translational Medicine, and Graduate Institute of Nanomedicine and Medical Engineering, College of Medical Engineering, Taipei Medical University, Taiwan

* These authors contributed equally to this work.

TAIPEI MEDICAL UNIVERSITY

Abstract

Steroid hormone and thyroid hormone exhibit different impacts on breast cancer. They bind to the respective receptors in the cytoplasm and form complexes, then translocate to the nuclei. In the nuclei, these hormone-receptor complexes bind to the promoters of genes responsive to these hormones. The transcribed genes respond to different cellular activities. In addition to their nuclear receptors, evidence indicates that steroid hormones and thyroid hormones can bind to cell membrane receptors. Integrin αvβ3 and other members of the integrin family which collaborate with extracellular proteins, are pivotal in regulating cell localization, mobilization, and signal transduction. Characteristics of cell type preferences suggest that integrin αvβ3 may be related to cancer cell growth and metastasis. Steroid hormone and thyroid hormones modulate breast cancer development via their nuclear receptors and integrin αvβ3. The molecular mechanisms involved in breast cancer cell growth include genomic and non-genomic functions of hormones. Modified integrin αvβ3 activities affect hormone-induced signal activation and downstream cellular biological activities. The integrin αvβ3 receptor for steroid hormones presents a wide range of cellular actions relevant to breast cancer biology, and the thyroid hormone analogs, tetrac and its derivatives, and other integrin αvβ3 inhibitors may help regulate these actions. To understand how steroid hormones interact with integrin αvβ3, computational binding modeling was carried out to explain the potential interactions of these hormones with the structure of integrin αvβ3. Gaining more insights into the binding modes of these hormones can significantly facilitate the design of specific integrin αvβ3 inhibitors for therapeutic purposes. Targeting integrins holds promise for the treatment of breast cancer that is refractory to hormonal therapy.

Introduction

1. Both steroid hormones and thyroid hormone induce closely related non-genomic and genomic signals.
2. Hormone-induced transcriptional changes require both processes to function normally. Non-genomic signaling can result from classic "nuclear" hormone receptors on or near the cell surface and other important signaling molecules on the cell membrane.
3. Integrin αvβ3 plays important roles in signal transduction, cell recruitment, and interactions with extracellular matrix proteins. It also functions as a receptor or binding site for steroid hormones and thyroid hormone.

Materials and Methods

Real-Time Quantitative Reverse Transcription PCR

Total RNA was extracted with genomic DNA removed by Illustra RNAspin Mini RNA Isolation Kit (GE Healthcare Life Sciences, Buckinghamshire, United Kingdom). 1 μg of DNase I-treated total RNA was reverse-transcribed using RevertAid H Minus First Strand cDNA Synthesis Kit (Life Technologies Corp.) into cDNA to use as the template for real-time PCR reaction and analysis. The real-time PCR reactions were conducted using QuantiNovaTM SYBR® Green PCR Kit (QIAGEN, Hilden, Germany) on CFX Connect™ Real-Time PCR Detection System (Bio-Rad Laboratories, Inc., Hercules, CA, United States). The reaction was conducted according to the manufacturer's instructions that an initial denaturation was at 95°C for 5 min, followed by 40 cycles of denaturing at 95°C for 5 s and combined annealing/extension at 60°C for 10 s. The primer sequences were as follows: *Homo sapiens integrin αv (ITGAV)*, forward 5'-TCC GAT TCC AAA CTG GGA GC-3' and reverse 5'-AAG GCC ACT GAA GAT GGA GC-3' (accession no.: NM_002210.4); *Homo sapiens integrin β3 (ITGB3)*, forward 5'-CTG GTG TTT ACC ACT GAT GCC AAG-3' and reverse 5'-TGT TGA GGC AGG TGG CAT TGA AGG-3' (accession no.: NM_000212.2); *Homo sapiens c-Myc*, forward 5'-TTC GGG TAG TGG AAA ACC AG-3' and reverse 5'-CAG CAG CTC GAA TTT CTT CC-3' (accession no.: NM_002467); *Homo sapiens CCND1*, forward 5'-CAA GGC CTG AAC CTG AGG AG-3' and reverse 5'-GAT CAC TCT GGA GAG GAA GCG-3' (accession no.: NM_053056); *Homo sapiens 18S ribosomal RNA (r18S)*, forward 5'-GTA ACC CGT TGA ACC CCA TT-3' and reverse 5'-CCA TCC AAT CGG TAG TAG CG-3' (accession no.: M10098)

Molecular Docking

The crystal structure of integrin αvβ3 was obtained from the Protein Data Bank (PDB ID: 1L5G). The chemical structures of cyclic RGD, Steroids, and thyroxine (T_4) were drawn using ChemBio3D Ultra 12.0. The molecules were docked with the integrin protein using Auto-Dock Vina. Grid box parameters were set up for integrin αvβ3 (center: x = 16, y = 43, z = 47; size: x × y × z = 45 × 45 × 45). The binding free energies (ΔG, kcal/mol) were calculated for each protein-ligand binding affinity. The docking results were visualized using PyMOL and analyzed using the BIOVIA Discovery Studio Visualizer to show the protein-ligand interactions.

Statistical Analysis

All of the collected data for nucleotide densities were analyzed by IBM®SPSS® Statistics software version 19.0 (SPSS Inc, Chicago, IL, United States). Student's t-test was also conducted. The p-values < 0.05 (*or#), and 0.01 (**or##) as the threshold for significance.

Results

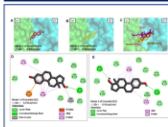

Fig. 1. Predicted docking poses of estradiol (E_2) bound at the cyclic Arg-Gly-Asp (cRGD)-binding site of integrin αvβ3. The docked protocol is according to a previous report. Docking modes 1 (A) and 2 (B) of estradiol (E_2) are colored red and yellow, and the free binding energies are anticipated to be of equal value of -6.9 kcal/mol. (C) Superimpositions of binding models for modes 1 (red) and 2 (yellow) mapped into the cRGD peptide (purple) of integrin αvβ3 subunits. Binding modes 1 (D) and 2 (E) of estradiol (E_2) are illustrated within integrin αvβ3 and their corresponding 2D interaction plots using the BIOVIA Discovery Studio Visualizer (http://accelrys.com).

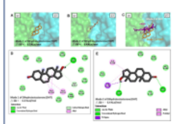

Fig. 2. Predicted docking poses of dihydrotestosterone (DHT) bound at the cyclic Arg-Gly-Asp (cRGD)-binding site of integrin αvβ3. The docked protocol was according to a previous report. Docking models 1 (A) and 2 (B) of DHT are respectively colored orange and wheat, and the free binding energies were anticipated to have values of -6.5 and -6.4 kcal/mol, respectively. (C) Superimpositions of binding models for modes 1 (orange) and 2 (wheat) mapped onto the cRGD peptide (purple) of αvβ3 integrin subunits. Binding modes 1 (D) and 2 (E) of DHT are illustrated within integrin αvβ3 and their corresponding 2D interaction plots by BIOVIA Discovery Studio Visualizer (http://accelrys.com).

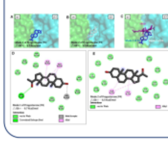

Fig. 3. Predicted docking poses of progesterone (P_4) bound at the cyclic Arg-Gly-Asp (cRGD)-binding site of integrin αvβ3. The docked protocol was according to a previous report. Docking models 1 (A) and 2 (B) of P_4 are respectively colored in blue and white, and the free binding energies are anticipated to be -6.7 -and -6.5 kcal/mol, respectively. (C) Superimpositions of binding models for modes 1 (blue) and 2 (white) mapped into cRGD peptide (purple) of integrin αvβ3 subunits. Binding modes 1 (D) and 2 (E) of P_4 are illustrated within integrin αvβ3 and their corresponding 2D interaction plots by the BIOVIA Discovery Studio Visualizer (http://accelrys.com).

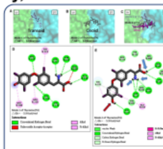

Fig. 4. Predicted docking poses of thyroxine (T_4) bound to the cyclic Arg-Gly-Asp (cRGD)-binding site of integrin αvβ3. The docked protocol is according to a previous report. Docking models 1 (A) and 2 (B) of T_4 are respectively colored in light blue and black, and the free binding energies were anticipated to have equal values of -5.9 kcal/mol. (C) Superimpositions of binding models for modes 1 (light blue) and 2 (black) mapped into the cRGD peptide (purple) of integrin αvβ3 subunits. Binding modes 1 (D) and 2 (E) of T_4 are illustrated within integrin αvβ3 and their corresponding 2D interaction plots by BIOVIA Discovery Studio Visualizer (http://accelrys.com).

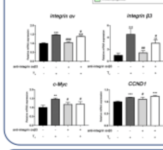

Fig. 5. T_4-induced gene expression is integrin αvβ3-dependent in breast cancer cells. MDA-MB-231 cells were treated with T_4 (10^{-7} M) in the presence or absence of anti-integrin αvβ3 anti-body for 24 hr. Cells were harvested. RNA was extracted and qPCR was conducted for quantifica-tion of integrin αv, integrin β3, c-Myc, and CCND1. Numbers of independent studies (n) = 3. **p < 0.01, ***p < 0.001, compared to the control; #p < 0.05, ##p < 0.01, ###p < 0.001, compared between T_4 treatment with or without ant-integrin αvβ3 antibody or between T_4 treatment and antibody treatment.

Conclusion

1. Molecular docking studies revealed that the binding domain of the Asp (D) residue of the cRGD ligand plays a pivotal role in interactions between hormones and the heterodimeric integrin αvβ3.
2. In addition, steroid hormones preferentially dock to the lower area of the cRGD site. These results are consistent with previous findings,
3. The thyroid hormone pocket is near the top of the cRGD recognition site, and the steroid hormone pocket is at the bottom of the cRGD domain.
4. Conveying a greater understanding of the intermolecular interactions can help in designing specific integrin αvβ3 inhibitors for therapeutic applications.
5. Non-genomic downstream integrin αvβ3 signaling regulates nuclear transcription through different pathways, including classical nuclear receptor localization and changes in the phosphorylation of key nuclear signaling molecules.
6. Understanding how genomic and non-genomic signaling works together to regulate important biological processes can help better design the regulation of these processes. It also can improve the possibility of treating hormone-dependent breast cancer and other tumors such as prostate cancer and lung cancer.

Funding

This work was supported in part by the TMU Research Center of Cancer Translational Medicine from The Featured Areas Research Center Program within the framework of the Higher Education Sprout Project, by the Ministry of Education (MOE) in Taiwan (DP2-107-20000), by TMU Research Center of Cancer Translational Medicine, Taipei Medical University, Taiwan, by a grant from the Ministry of Science and Technology, Taiwan (MOST 111-2314-B-038-123 to HY Lin), and by an integrated grant from the Ministry of Science and Technology, Tai-wan (NSTC 112-2314-B-038-004 to HY Lin).